

THE EFFECT OF PLY ORIENTATION ON THE VIBRATION CHARACTERISTICS OF 'T' STIFFEN COMPOSITES PANEL: A FINITE ELEMENT STUDY

Opukuro S David-West^{1*}

Division of Automotive, Mechanical and Mechatronics Engineering,
School of Engineering and Technology, University of Hertfordshire,
Hatfield, United Kingdom, AL10 9AB

ABSTRACT

Aircraft producers have extensively adopted the use of T-shaped stiffened fibre reinforced composite panels in the thin walled structures such as the fuselage and wings. The composite materials present the advantage of high specific strength and stiffness ratios, coupled with weight reduction compare to traditional materials. This report presents a numerical study about the free-free vibration analysis of T-stiffened carbon fibre reinforced epoxy composite panels with surface and identical ply orientations of 0°, 15°, 30°, 45°, 60°, 75° and 90° using ANSYS 17 finite element code. These changes has effect on the element stiffness matrix and hence the dynamic characteristics of the panels. The fundamental frequencies increase to a peak and then decrease taking the form a half sine curve. The dynamic analysis was realized using the Lanczos tool to extract the mode shapes and natural frequencies.

KEYWORDS: *Stiffen pane; Modal analysis; Finite element analysis; Composite structure*

1.0 INTRODUCTION

The desire of light weight structures in the aerospace industries in the present day advanced technology has increasingly admitted the use of composite materials in the secondary structures such as the fuselage, wing, engine cowl, landing gear cover, rudder, control surfaces, cabinets etc. Stiffened composite panels reinforced with 'T' stiffeners are used in the construction of aircraft wings. The composite skin and stiffener laminates consist of layers stacked at different fibre orientation angles, which are often limited to 0°, 45°, and 90° (Liu, et al 2010). The 45° plies are suitable to absorb the shear loads. The use of stiffened panels contributes to reduction in the weight of the panel without compromising the strength and stiffness.

(York & Williams, 1998), determined the critical buckling loads of prismatic benchmark metal and composite panels representative of typical aircraft wing panel configurations, with in-plane shear and compression load combinations using exact' and

*Corresponding author e-mail: o.david-west@herts.ac.uk

approximate methods. While (Rikards, et al 2001) developed triangular finite element model for buckling and vibration analysis of laminated composite stiffened shells. Also (Suh, et al 2003) investigated the damage tolerance of stitched stiffened composite panels with clearly visible impact damage and discussed about the effects of stitching using unstitched, selectively stitched and fully stitched panels. (Chiarelli, et al 1996) discussed about the post critical characteristics of stiffened panels loaded in compression and design strategies in this regime. While (Chen, et al 2003) presented an analytical method for ultimate longitudinal strength calculation and reliability analysis of a ship's hull made of composite materials.

The definition of a post-buckling optimisation procedure for the design of composite stiffened panels subjected to compression loads was reported by (Bisagni & Lanzi, 2002) based on a global approximation strategy, where the structure response is given by a system of neural networks. (Beton & Amadio, 2012) presented an analytical formulation proposed for the estimation of the buckling resistance of flat laminated glass panels under in-plane compression or shear, using two different design approaches one directly derived from the theory of sandwich panels and the other based on the approximate concept of equivalent thickness.

(Hwang & Huang, 2005) employed nonlinear buckling analysis using the finite element method to investigate buckling and postbuckling behaviour of unidirectional composite materials with two delaminations under uniaxial compression and reported that with a long delamination close to the surface of the laminate, the inner and short delamination has no effect on the buckling stress. However, the presences of inner, short delamination significantly change the behaviour of delamination growth. (Lanzi & Giavotto, 2006) presented a multi-objective optimization procedure for the design of composite stiffened panels based on Genetic Algorithms and three different methods of global optimization: Neural Networks, Radial Basis Functions and Kriging approximation, and the response surfaces were used to approximate the post-buckling characteristics.

Research of fatigue and stability of the highly stressed thin plate structures is an ongoing activity that provides valuable information for the structural engineers. (Jia & Ulfvarson, 2004) investigated about the static and dynamic behaviour of a lightweight ship deck and reported about the improvement that can be achieved by replacing a conventional steel structure with lightweight material using finite element. The free vibrations characteristics of simply supported anisotropic composite laminates were investigated using analytical approach (Ganapathi, et al 2009) using the first-order shear deformation theory and the shear correction factors. (Yang, et al 2008) investigated the reliability of orthogonally stiffened composite plate with boundary conditions of all four edges simply supported to uniform transverse load using grillage model assumptions and sensitivity of the variables observed.

(Sliseris & Rocens, 2013) proposed an optimization technique for composite plates with discrete varying stiffness consisting of three steps for structural compliance and stress field differences, size optimization with genetic algorithm and dimension optimization of plates internal structure by neural network. (Herencia, et al 2008) presented an initial sizing optimisation of anisotropic composite panels with T-shaped stiffeners using mathematical programming to model the skin and the stiffeners with the laminate

parameters and genetic algorithms to account for manufacturability and design practices.

(Xue, et al 2011) investigated about the optimization of top-hat stiffened composite panels with the objective to minimize the weight and concluded from the parametric study that the plate aspect ratio and in-plane loading ratio have coupling effects on the critical buckling load. (Marín, et al 2012) reported the optimization procedure for a geometric design of a composite material stiffened panel by a neural network system using the results of finite element analyses and genetic algorithm. The composite panels considered in this investigation have the longitudinal stiffeners, loaded in the in-plane direction, with changes to the surface and identical ply orientation being 0° , 15° , 30° , 45° , 60° , 75° and 90° , which has effect on the laminate stiffness and hence the vibration characteristics. The angle plies are known to support the structure against shear loading, but commonly reported in the literatures are laminates that contains the $\pm 45^\circ$ plies; in this investigation other additional angle plies have been considered i.e. $\pm 15^\circ$, $\pm 30^\circ$, $\pm 60^\circ$ and $\pm 75^\circ$. The results of this study will be useful to the manufacturers and users of stiffened panels such as the aerospace industries.

2.0 DESCRIPTION OF THE PANEL

The structure being used for this investigation has the special design such as the ones application for use at the wings of the aircraft. The sketch of the panel is shown in Figure 1 showing the skin, web and foot-flange as parts of the structure. The stringer consists of the web and the foot-flange. All the parts of the panel are made of carbon fibre reinforced epoxy composite material. The stringer being perfectly bonded to the skin with epoxy as the adhesive which is the same material as the base resin of the composites laminate that comprises all the component parts. The stringers strengthen the skin and keeping it stable so it can absorb in-plane load.

The laminate configurations of the components of the panels are as described in Table 1. The thickness of a ply was 0.125 mm. The strength of the panel will depend on the laminate configuration of the component parts, bonding strength between the foot-flange and skin, and the manufacturing process. These carbon fibre reinforced composite panels have superior strength and stiffness compared to ones made with traditional materials such as steel or aluminium. Also it is lighter in weight, making it a good candidate for air vehicles. The uniqueness of the panel construction provides resistance to impact blow, vibration and breakage. About 50% of aircraft structures are made of carbon fibre reinforced composite materials (Roeseler, et al 2007). Also (Tanasa & Zanoaga, 2013) has document reasons as regards the continuous use of carbon fibre-reinforced composites in the aviation industry. In Boeing 787, (Nayak, 2014) some of the components of the wings are made of carbon fibre reinforced composites; the stacking plies typically comprises of 0° , 90° , 45° and -45° directions (Liu, et al 2010). The 0° and 90° plies are useful to take the in-plane loads, while the $\pm 45^\circ$ plies supports the shear strength.

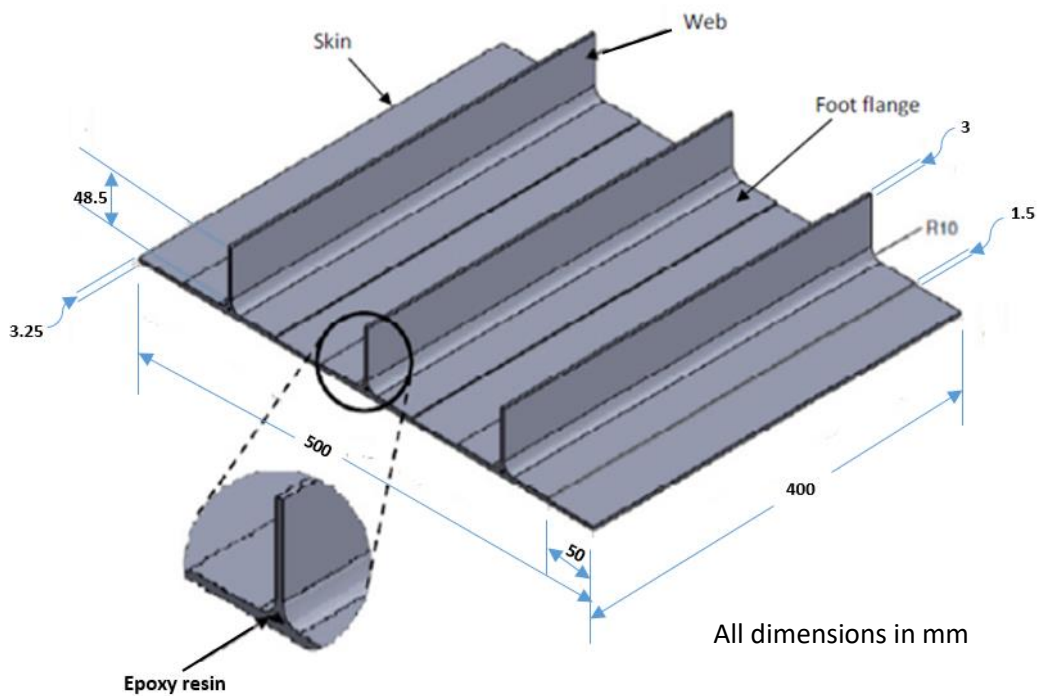


Figure 1. Features of the T-stiffened composite panel.

Table 1: Laminate configurations of the panels

Description	Lay up
Skin	$[A^\circ/0^\circ/-A^\circ/A^\circ/90^\circ/0^\circ/\pm A^\circ/0^\circ/-A^\circ/A^\circ/90^\circ/-A^\circ]_s$
Web	$[A^\circ/0^\circ/90^\circ/-A^\circ/90^\circ/0^\circ_2/90^\circ/-A^\circ/90^\circ/0^\circ/A^\circ]_s$
Foot flange	$[A^\circ/0^\circ/90^\circ/-A^\circ/90^\circ/0^\circ]_s$

where $A = 0^\circ, 15^\circ, 30^\circ, 45^\circ, 60^\circ, 75^\circ$ and 90°

3.0 MATERIAL PROPERTIES

The material used for the composite structure is carbon fibre reinforced / epoxy lamina. The unidirectional layer orthotropic properties for the material are given as in Table 2, as obtained from reference (Hou, et al 2000) were used in the finite element analysis.

Table 2: Material properties for CFRP composite lamina

Property	Value
E_x (GPa)	132
E_y (GPa)	10.3
E_z (GPa)	10.3
G_{xy} (GPa)	6.5

G_{xz} (GPa)	6.5
G_{yz} (GPa)	3.91
ν_{xy}	0.25
ν_{xz}	0.25
ν_{yz}	0.38
ρ (kg/m ³)	1570

The material properties are given with reference to the ply coordinate axes where index 'x' denotes the ply principal axis that coincides with the direction of maximum in-plane Young's modulus (fiber direction). Index 'y' denotes the direction transverse to the fiber in the plane of the lamina and index 'z' the direction perpendicular to the plane of the lamina. The lamina is a transversely isotropic structure, hence where E_x represent the Longitudinal Modulus, E_y and E_z the Transverse Modulus, ν_{xy} is the major Poisson's Ratio and G_{xy} , G_{xz} and G_{yz} are in-plane Shear Modulus.

Table 3: The specifications of epoxy properties

Property	Value
Modulus, E (GPa)	10.5
Poisson's ratio, ν	0.3
Density, ρ (kg/m ³)	1560

In Table 3 are the mechanical properties of the resin used for the analysis used to characterise the solely resin rich sections of the model.

4.0 CONCEPT OF DYNAMIC ANALYSIS

A general dynamic analysis will solve the equation of motion which gives the time dependent response of every node point in the structure by including inertial forces and damping forces in the equation.

$$[M]\{\ddot{x}\} + [C]\{\dot{x}\} + [K]\{x\} = \{F\} \quad (1)$$

where $[M]$ represents the structural mass matrix, $\{\ddot{x}\}$ the nodal acceleration vector, $[C]$ the structural damping matrix, $\{\dot{x}\}$ the node velocity vector, $[K]$ the structure stiffness matrix, $\{x\}$ the node displacement vector and $\{F\}$ is the applied time varying load.

Most engineering systems designers are interested in the natural frequencies and mode shapes of vibration of the system. However, for vibration modal analysis, the damping is generally ignored and considering a free vibration multi-degree of freedom system, the dynamic equation becomes.

$$[M]\{\ddot{x}\} + [K]\{x\} = \{0\} \quad (2)$$

If the displacement vector $\{x\}$, has the form $\{x\} = \{X\} \sin \omega t$, then the acceleration vector is $\{\ddot{x}\} = -\{X\} \omega^2 \sin \omega t$ and substituting into equation (2), gives the eigenvalue equation.

$$([K] - \omega^2 [M])\{X\} = \{0\} \quad (3)$$

Each eigenvalue has a corresponding eigenvector and the eigenvectors cannot be null vectors.

$$|[K] - \omega^2 [M]| = 0 \quad (4)$$

Equation (3), represent an eigenvalue problem, where ω^2 is the eigenvalue and $\{X\}$ the eigenvector (or the mode shape). The eigenvalue is the square of the natural frequency of the system.

5.0 GEOMETRY OF THE SHELL ELEMENT AND THE STRESS – STRAIN RELATIONSHIP

ANSYS Shell281 element was primarily used to model the composites plates; it is primarily used to model composite shells or sandwich construction. The accuracy in modelling composite shells is governed by the first-order shear-deformation theory (usually referred to as Mindlin-Reissner shell theory). The element is formulation based on logarithmic strain and true stress. The element has eight nodes with six degrees of freedom at each node, i.e. translations in the x, y, and z axes, and rotations about the x, y, and z-axes. Figure 2 shows the geometry and node locations of the element. It is defined by shell section information and eight nodes (I, J, K, L, M, N, O and P). A triangular-shaped element may be formed by defining the same node number for nodes K, L and O as shown in Figure 2.

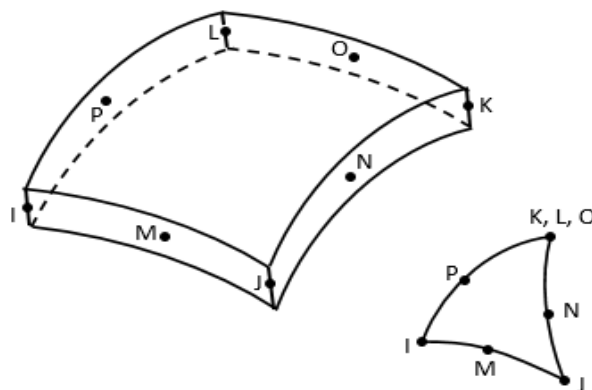


Figure 2. Geometric description of shell281 (ANSYS, 2103).

The stress is related to the strains by:

$$\{\sigma\} = [D]\{\varepsilon\} \quad \text{or} \quad \{\varepsilon\} = [D]^{-1}\{\sigma\} \quad (5)$$

This is in accordance with the Hooke's law.

The flexibility or compliance matrix, $[D]^{-1}$ is (ANSYS, 2013)

$$[D]^{-1} = \begin{bmatrix} 1/E_x & -\nu_{xy}/E_x & -\nu_{xz}/E_x & 0 & 0 & 0 \\ -\nu_{yx}/E_y & 1/E_y & -\nu_{yz}/E_y & 0 & 0 & 0 \\ -\nu_{zx}/E_z & -\nu_{zy}/E_z & 1/E_z & 0 & 0 & 0 \\ 0 & 0 & 0 & 1/G_{xy} & 0 & 0 \\ 0 & 0 & 0 & 0 & 1/G_{yz} & 0 \\ 0 & 0 & 0 & 0 & 0 & 1/G_{xz} \end{bmatrix} \quad (6)$$

E_x = Young's modulus in the x-direction; E_y = Young's modulus in the y-direction
 E_z = Young's modulus in the z-direction; ν_{xy} = major Poisson's ratio; ν_{yx} = minor Poisson's ratio;
 ν_{xz} = major Poisson's ratio X-Z plane; G_{xy} = shear modulus in the xy plane
 G_{yz} = shear modulus in the yz plane; G_{xz} = shear modulus in the xz plane

Also, the $[D]^{-1}$ matrix is assumed to be a symmetric matrix, so that:

$$\frac{\nu_{yx}}{E_y} = \frac{\nu_{xy}}{E_x} \quad ; \quad \frac{\nu_{zx}}{E_z} = \frac{\nu_{xz}}{E_x} \quad ; \quad \frac{\nu_{zy}}{E_z} = \frac{\nu_{yz}}{E_y}$$

In fibre reinforced composite structures the stiffness is affected by the stacking sequence and hence the stiffness matrix of equation (4) for the eigenvalue analysis. A component of the stiffness is the $[D]$ which consist of the modulus and the poison's ratio.

6.0 FINITE ELEMENT MODELLING AND THE MESH DISCRETIZATION

A three-dimensional linear elastic finite element model of the composite panel was constructed using Shell 281 (element with mid-side node) in ANSYS 17 finite element code. This element has six degrees of freedom at each node. The discretisation is the splitting of the continuous composite panel into the attached separated units. The finite element model has 5960 shell elements and 360 solid elements for all the panels considered in this study.

Figure 3 shows the finite element discretisation for the panel with the display of the shell element thickness. The element size was 10 mm. The epoxy resin rich region between the web, foot flange and skin was characterised using a solid element with corner and mid-side nodes (Solid 186) and the contact between the foot flange and skin as bonded model.

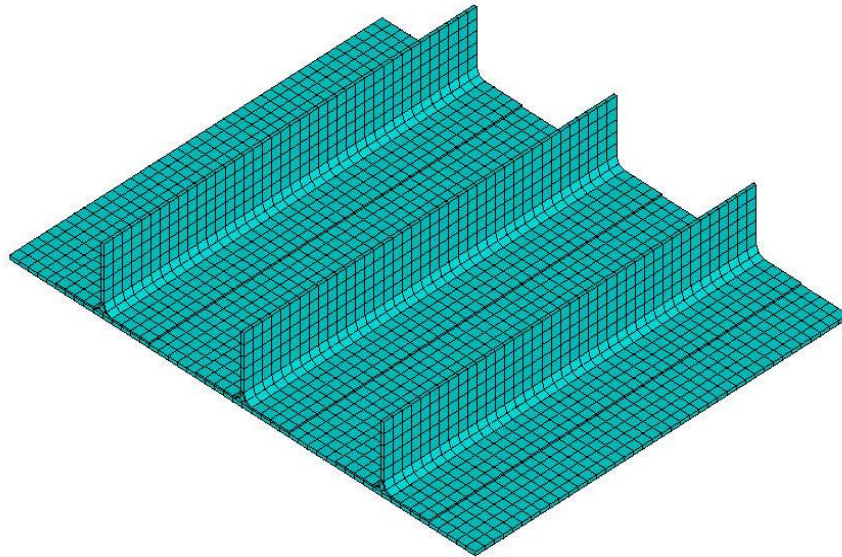


Figure 3. Mesh discretization of the panel showing the display of the elements

The shell element allows for finite rotations and membrane strains. The models were discretized into sufficient number of elements to allow for adequate representation of the deformation that coincides with the natural frequencies of the panels.

7.0 MODAL ANALYSIS OF COMPOSITE PANELS

The aim of the modal analysis is to determine the natural mode shapes and frequencies of the panel during free vibration. The mode shapes describe the deformation of the structure at the natural frequencies. This resonant vibration is usually due to the interaction between the inertial and elastic properties of the panel materials. The analysis was performed using modal analysis tool available in ANSYS 17 finite element code.

The first twenty-one modes of vibration of the panels were extracted using the Block Lanczos method. As this is a free vibration analysis i.e. no boundary condition, and the elements in it description have six degrees of freedom at each node, the first six modes were rigid body modes with zero frequency value. The finite element analysis yields a stiffness matrix and a mass matrix; with these two matrices (while the damping effect is ignored) an eigenvalue problem is generated and solved for the mode shapes and natural frequencies of the panels. Usually, it is a good idea to design the panels operating below the fundamental frequency (i.e. the first mode).

8.0 DESCRIPTION AND COMPARISON OF FUNDAMENTAL MODE SHAPES

The mode shapes were affected by the characteristics of the structure such as the stiffness, deflection distribution and fiber orientation. The laminates that constitute the panels are symmetrical in the stacking sequence, but the difference being the orientation of the surface ply and identical lamina, which are 0° , 15° , 30° , 45° , 60° , 75° , and 90° , Table 1 shows the stacking sequence. In Figures 4 to 10 are the fundamental modes of vibration with the natural frequencies of 41 Hz, 54 Hz, 65 Hz, 74 Hz, 71 Hz, 55 Hz and 42 Hz respectively.

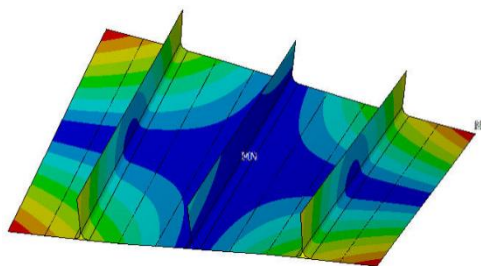


Figure 4. 0° degree surface ply orientation

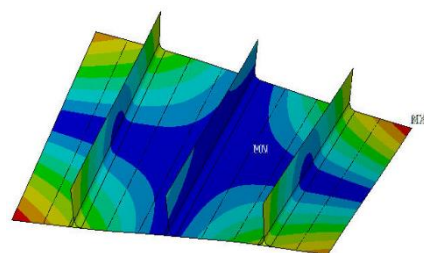


Figure 5. 15° degree surface ply orientation

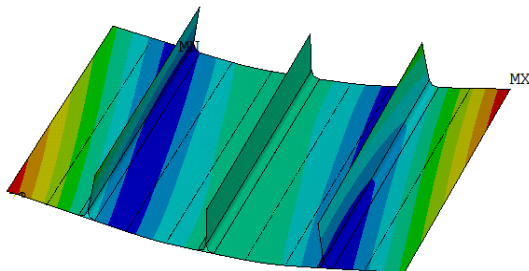


Figure 6. 30° degree surface ply orientation

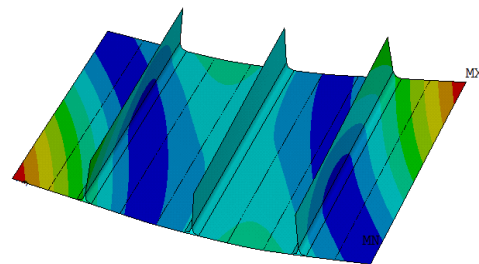


Figure 7. 45° degree surface ply orientation

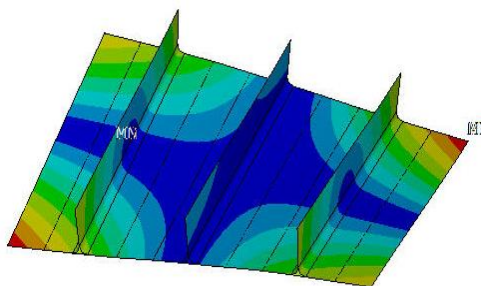


Figure 8. 60° degree surface ply orientation

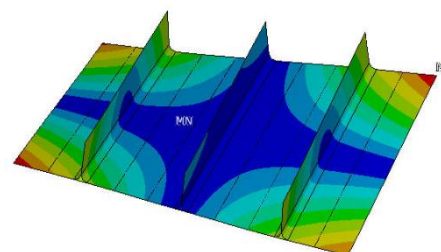


Figure 9. 75° degree surface ply orientation

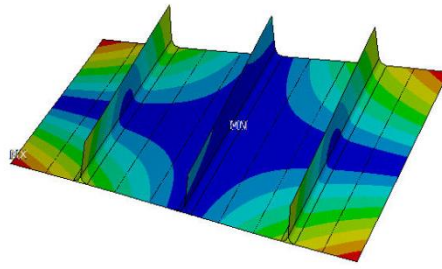


Figure 10. 90° degree surface ply orientation

Exploring the mode shapes of the stiffened plate it could be seen that the fundamental modes for the panels with 0°, 15°, 60°, 75° and 90° surface ply orientation are similar. Much of the vibration energies seems to have been trapped at the corners where the maximum displacements were attained. This implies that the corners of the panels were compliant with the energy at the fundamental frequencies. The shear effects were pronounced in the panels with the 30° and 45° surface ply directions, hence suitable configuration for the absorption of shear loads. The maximum displacements are trapped at two opposite corners of the panels.

9.0 THE EFFECT OF SURFACE PLY ORIENTATION

The vibration of the composite panels depends highly on the extremely large number of material permutations, such as the stacking sequence, architecture and the interface properties. Hence, the strategies to achieve the design requirements must take into account the complexities of composite material structure and the geometry of the structural elements. Axially biased composite laminates such as the ones of the panels consider in this study are an important class of laminates as they display good characteristics in both the axial and shear directions. They are favoured in the design of structures in the aerospace, marine and automobile industries, depending on how the designers want to tailor the strength properties.

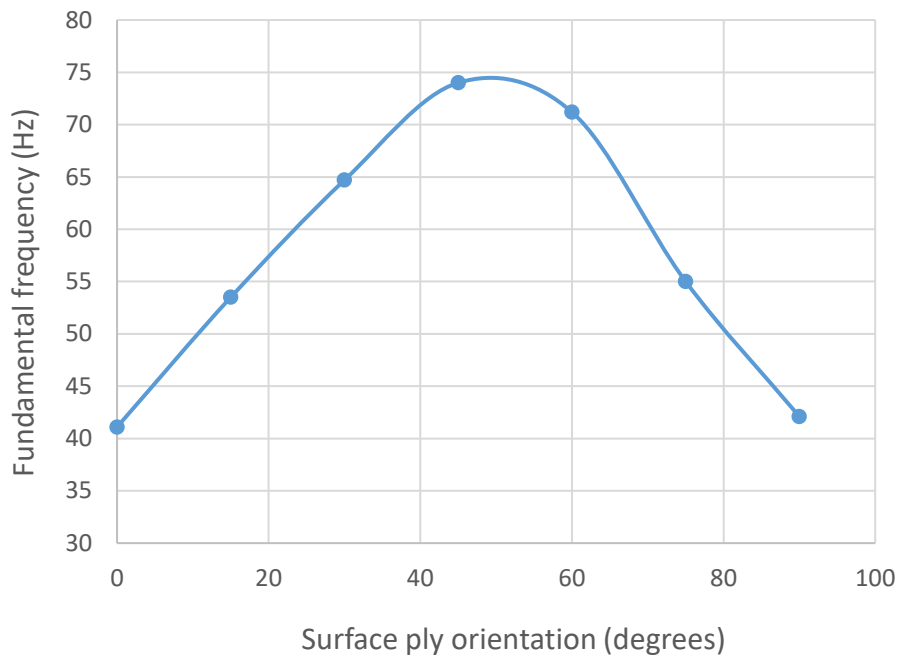


Figure 11. The relation between the fundamental frequency and the surface ply orientation

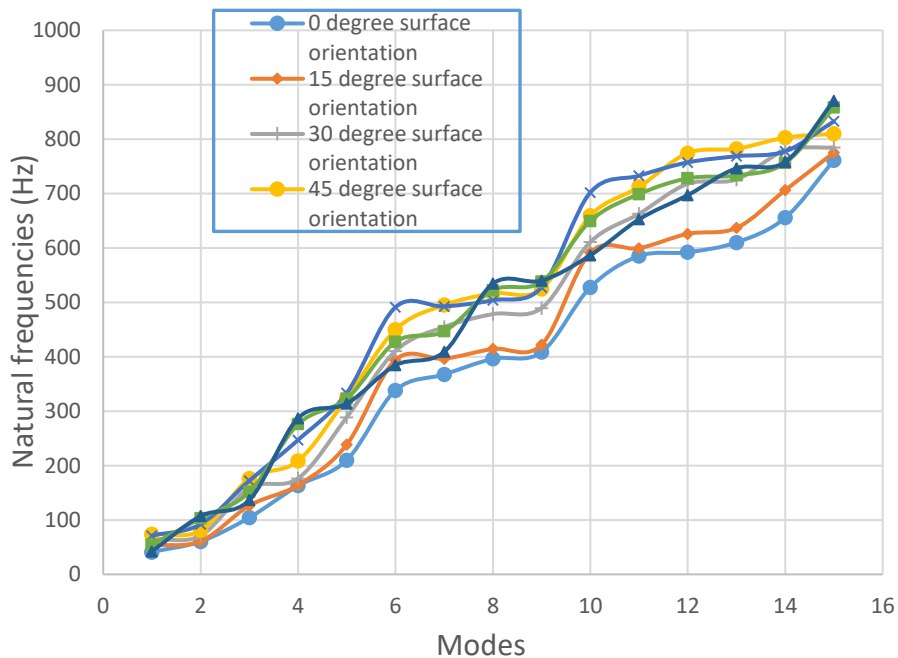


Figure 12. Comparison of the natural frequencies

In Figure 11 is presented the plot of the fundamental frequencies of the panels as against the surface ply fibre direction. The curve takes the form of an approximate half sine

curve with fundamental frequencies increase from 0° to 45° surface ply panels and decrease from the 60° to 90° surface ply direction panels. The highest value of the first natural frequency being 74 Hz, attributed to the panel with 45° direction for the surface lamina is indicative of the fact that it has the highest stiffness.

The relationships between the natural frequencies and the modes for all the panels are plotted and superimposed in Figure 12. It is an approximate step-wise rise from the lowest to the highest value. The differences become significant as the resonant frequencies increases, this is thought be because of the laminate stacking sequence that has significant effect on the panel stiffnesses and the complex vibration energy absorption characteristics at high frequencies. These fourteen natural frequencies of the panels ranging from 41 – 761 Hz, 53 – 775 Hz, 65 – 785 Hz, 74 – 810 Hz, 71 – 832 Hz, 55 – 859 Hz and 42 – 871 Hz for the 0°, 15°, 30°, 45°, 60°, 75° and 90° surface ply direction panels respectively.

10.0 CONCLUSIONS

This study has shown that surface ply orientation of carbon fibre reinforced composite panels and stacking sequence have significant effect on the vibration performance of the structure. The natural frequencies of vibration and the mode shapes of the panels were obtained by using the Lanczos tool to extract the dynamic characteristics. Some of the modes have the vibration energies trapped at certain locations of the panel, while others were globally.

The first natural frequencies of the panels changes as the ply direction at the surface of the panels and identical lamina changes from 15° to 90°. An increase to a peak value of 74 Hz for the panel with 45° on the surface and then gradually decreases. Also considering the relationship of how the first fifteen natural frequencies increases with the modes an approximate step-wise rise from the lowest to the highest value was observed. As the configurations of the composite panels used for this study are typical for the aerospace industries, these results from this investigation will be of interest to such industries. Further investigation in this study will be to see the effect of hybridization. This work has implications in the selection of composite laminate lay up for optimum combinations stiffness, vibration, compression and shear behaviour.

REFERENCES

ANSYS Mechanical APDL Theory Reference 2013.

Bedon, C., & Amadio, C. (2012). Buckling of flat laminated glass panels under in-plane compression or shear. *Engineering Structures* 36 185–197.

Bisagni, C., & Lanzi, L. (2002). Post-buckling optimisation of composite stiffened panels using neural networks. *Composite Structures* 58 237–247.

- Chen, N. Z., Sun, H., & Guedes Soares, C. (2003). Reliability analysis of a ship hull in composite material. *Composite Structures* 62, 59–66.
- Chiarelli, M., Lanciotti, A., & Lazzeri, L. (1996). Compression behaviour of flat stiffened panels made of composite material. *Composite Structures* 36, 161 – 169.
- Ganapathi, M., Kalyani, A., Mondal, B., & Prakash, T. (2009). Free vibration analysis of simply supported composite laminated panels. *Composite Structures* 90, 100–103.
- Herencia, J. E., Weaver, P. M., & Friswell, M. I. (2008). Initial sizing optimisation of anisotropic composite panels with T-shaped stiffeners. *Thin-Walled Structures* 46, 399–412.
- Hou, J. P., Petrinic, N., Ruiz, C., & Hallett, S. R. (2000). Prediction of impact damage in composite plates. *Composites Science and Technology* 60 273 - 281.
- Hwang, S., & Huang, S. (2005). Postbuckling behavior of composite laminates with two delaminations under uniaxial compression. *Composite Structures* 68, 157–165.
- Jia, J., & Ulfvarson, A. (2004). A parametric study for the structural behaviour of a lightweight deck. *Engineering Structures* 26, 963–977.
- Lanzi, L., & Giavotto, V. (2006). Post-buckling optimization of composite stiffened panels: Computations and experiments. *Composite Structures* 73, 208–220.
- Liu, D., Toropov, V. V., Zhou, M., Barton, D. C., & Querin, O. M. (2010). Optimization of blended composite wing panels using smeared stiffness technique and lamination parameters. In *Proceedings of the 51st AIAA/ASME/ASCE/AHS/ASC Structures, Structural Dynamics, and Materials Conference*, Orlando, Florida, 12 April 2010 - 15 April 2010.
- Marín, L., Trias, D., Badalló, P., Rus, G., & Mayugo, J.A. (2012). Optimization of composite stiffened panels under mechanical and hygrothermal loads using neural networks and genetic algorithms. *Composite Structures* 94, 3321–3326.
- Nayak, N. V. (2014). Composite materials in aerospace applications. *International Journal of Scientific and Research Publications*, Volume 4, (9), 2250-3153.
- Rikards, R., Chate, A., & Ozolinsh, O. (2001). Analysis for buckling and vibrations of composite stiffened shells and plates. *Composite Structures* 51 361 – 370.
- Roeseler, W. G., Sarh, B., & Kismarton, M. U. (2007). Composite Structures: The First 100 Years. In *Proceedings of the 16th International Conference on Composite Materials*, Kyoto, Japan, 8 – 13 July 2007.

- Sliseris, J., & Rocens, K. (2013). Optimal design of composite plates with discrete variable stiffness. *Composite Structures* 98, 15–23.
- Suh, S. S., Han, N. L., Yang, J. M., & Hahn, H. T. (2003). Compression behavior of stitched stiffened panel with a clearly visible stiffener impact damage. *Composite Structures* 62, 213–221.
- Tanasa, F., & Zanoaga, M. (2013). Fibre-reinforced polymer composites as structural materials for aeronautics. In *Proceedings of the International Conference of Scientific Paper, Brasov, 23 – 25 May 2013*.
- Xue, X. G., Li, G. X., Sheno, R. A., & Sobey, A. J. (2011). The Application of Reliabilitybased Optimization of Tophat Stiffened Composite Panels Under Bidirectional Buckling Load. In *Proceedings of the 18th International Conference on Composite Materials, South Korea, Jeju Island, 21 – 26 August 2011*.
- Yang, N., Das, P. K., & Yao, X. (2008). Reliability analysis of stiffened composite panel”. In *Proceedings of the 4th International ASRANet Colloquium, Athens, 2008*.
- York, C. B., & Williams, F. W. (1998). Aircraft wing panel buckling analysis: efficiency by approximations. *Computers and Structures* 68, 665 – 676.